Indian Journal of Engineering & Materials Sciences
Vol. 30, December 2023, pp. 845-853
DOI: 10.56042/ijems.v30i6.4581

Optimization of Anode Electrode Resistance using Synthesised Graphene Oxide for DSSC Aplications

Hirasing T Manza[a], Mangesh S Dhore*[a], Shankar Amlraj[a], Ramesh Pugalenthi[a]
[a]G H Raisoni University, Anjangaon Bari Road, Amravati 444 701, India
[b]Karunya Institute of Technology and Sciences, Karunya Nagar, Tamilnadu 641 114, India

Received: 17 June 2023; Accepted; 18 October 2023

The graphene oxide is synthesized by modified hummer's method. The purification process is done by electrochemical and physical methods. UV Visible, FT-IR, and Raman Spectroscopy characterize the resulting synthesized material. The surface morphology of the wrinkled paper shape is found by SEM and the size of the particles is determined by HR-TEM techniques. The layer distance between the starting material and the final product is calculated by XRD analysis. Through TGA analysis, it is found that the developed material is more stable at higher temperature and subsequently, it tends to be utilized in DSSC applications. The developed GO is coated on a glass plate using the spin coating technique with annealing to convert the normal glass into the conductive glass. And that conductive glass is used as a counter electrode for DSSC. The optimization of electrode resistance is done with the same annealing process by varying the temperature and the number of coatings.

Keywords: GO-Graphene oxide, Spectral Technique, DSSC- Dye-Sensitized Solar Cell

1 Introduction

Now a days graphene is a sensational material. Graphene is having SP_2 hybridized carbon atoms with hexagonal shape[1]. It is synthesized in different layered forms i.e. monolayer, bilayer, and multi-layer. Since it is having versatile properties of a larger specific surface area[2], thermal conductivity[3], high electron mobility[4], high electrical conductivity, and Young's modulus[5], it can be applied in various fields like energy storage devices, advanced targeted drug delivery, coating materials, sensors, etc. The Young's modulus of graphene alone is more than two TPa[6] which is ten times higher than normal steel material[7]. In the present research, graphene oxide is synthesized by the Hummers method for applications of DSSC.

Human activities are overloading the earth with emissions of carbon leading to global warming. Subsequently, it is gearing up the planet's temperature. This causes adverse effects on the entire ecosystem with higher impacts on human health, environment, and climate changes[8]. Among all the energy resources, electrical energy generation with fossil fuels is the main cause of the emissions[9]. To curb emissions, the entire world is moving towards renewable sources like wind, solar, and hydro energy sources. As hydropower and wind power are seasonal, their production reliability is low, and they are subjected to various environmental constraints. From the economic investment point of view, wind and solar power plants require huge capital costs and take a long time to return on investment time[10]. So, scientists are turning towards affordable and cheaper technologies to overcome the higher investment cost. So in this research, the focus is given to solar energy production. So far, solar energy production has been entirely based on silicon material-based p-n junction diode devices. The major advantage of silicon is in its lower cost and abundance. The added advantage of silicon photovoltaic devices is that they are stable when we combine the research into practical systems[11]. The disadvantage of silicon photovoltaic devices is that they should be purely manufactured from silicon material. The purity level should be at its maximum and the added purification cost makes it very expensive as compared to non-renewable energy technologies. Moreover, dumping the wasted solar panel is also critical. So the energy sector and researchers are keen to look into the next generation of solar cells that are free from silicon. Michael Grätzel's band, Brian O'Regan in 1988 at UC Berkeley invented non-silicone material named as DSSC[12]. It comprises anode, cathode, and in-between

*Corresponding author (E-mail: mangeshdhore2@gmail.com)

dye as electrolytes[13]. The Dye-sensitized solar cell is a pathway mimicking the process of photosynthesis. And it has the advantages of being less expensive, eco-friendly, using cheaper technology, etc.[14] The DSSC assembly is comprised of the metal oxide semiconductor, the conductive counter electrode, sensitized dye, and a redox couple electrolyte. The electrical or electronic load can be connected externally between the metal oxide semiconductor and the counter electrode. The combination of the redox couple and the dye molecule is kept between the package structures of DSSC. There are various metal semiconductors like ZnO, TiO_2, and SiO_2 are used in the fabrication of DSSC as a cathode. In the present study, titanium dioxide is used as a cathode because of the higher and more robust benefits of lower cost, abundance in nature, non-toxicity, and higher stability[15]. As in DSSC, several dyes are used along with redox couples, such as chlorophyll, betanins, carotenoids, anthocyanins, and various synthetic dyes. Strong bonding is fundamentally required between the dye and the cathode for the enhanced efficiency of DSSC. Additionally, the dye is expected to have more absorption in the visible region of the spectrum[16]. The anode should be coated with a conductive material with higher stability. As the conductivity of RGO is higher than that of GO, it is the best choice available to coat the anode glass material. But the RGO cannot be coated with the anode glass material directly. So that the synthesized GO is coated on the glass material through the spin coating method. The layer formation of graphene is established after sintering at higher temperatures beyond 200 °C in a muffle furnace. As we know, the GO will be reduced to RGO after 200 °C. So naturally, the coating of RGO in anode glass material is established by spin coating and sintering of GO in the glass material.

2 Materials and Methods

2.1 General characterization

X-ray diffraction patterns were recorded on a Shimadzu XRD-6000 powder X-ray diffractometer at 40 kV voltage and 30 mA current. Fourier transform infrared spectra (FT-IR) were recorded on an IR-Prestise-21 Shimadzu. Raman spectra were recorded on a Horiba-Jobin Raman spectrometer with a 514 nm laser at a power. TGA measurements were carried out under an N_2 atmosphere using a NETZSCH STA 449 F3 Jupiter. High-resolution transmission electron microscopy (HR-TEM) and selected area electron diffraction (SAED) measurements were conducted on a JEOL JEM-2100 for the surface morphology of GO. Scanning electron microscopy (SEM) images were recorded on an ESEM FEI QUANTA 200.

2.2 Synthesis of graphene

In this research, graphene oxide was synthesized by using the Hummers method for the development of an anode of DSSC[17-18]. Accordingly, 3 g of graphite powder was added to the solution comprising 1.5 g of sodium nitrate followed by 69 ml of a 98% solution of sulphuric acid and the mixture was stirred for about 30 minutes in an ice bath at 0 °C. Subsequently, 9 g of potassium permanganate was slowly added to the stirring reaction mixture and the temperature was allowed to rise gradually to 20 °C in 30 minutes then to 40 °C. After about 90 minutes 46 mL of DI water was added and the temperature was further increased to 90 °C for 15 minutes. To dilute the reaction mixture further, addition the prepared solution is added to 140 mL of DI water. After some time with the reaction mixture, 3 mL of 30% H_2O_2 was added until the color of the suspension in the mixer reaches yellow. Subsequently, the mixture was added to a 100 mL of D.D. water until it reaches a brown color. The obtained suspension was washed with 5% HCl and D.D. water. The dispersed GO was separated by centrifugation at 3000 rpm for 10 min. After removing exfoliated graphite and other impurities, the product is kept in the oven for a night at 60^{o} C[19-20] the product is ready for further experiments.

2.3 Preparation of the anode

The synthesized graphene oxide was mixed with water and continuously stirred for twenty minutes to get graphene oxide dispersion. The dispersed solution is taken in a pipet, and it is coated in glass material through spin coating and sintering further with annealing. The coating process is done at different temperatures, between 100-400 ^{o}C. For every coating, the resistance is measured with different coatings at different temperatures. The optimum resistance is found at the fourth coating at 240 ^{o}C.

2.4 Preparation of cathode material

The preparation of the cathode is done with the binding of TiO_2 paste and the conductive glass. The TiO_2 paste is prepared by mixing acetic acid and TiO_2 coated on the conductive glass by the doctor's blade method. The coated TiO_2 glass material is kept at

room temperature for some time, and then it is sintered in a hot oven (40–50 °C) until the color of the material changes from white to brown for effective binding of TiO_2 with conductive glass material. The particle size of the TiO_2 was kept less than 40nm to avoid peeling off of TiO_2 during the preparation of the solar cell. The annealing process was carried out until the material was coated on the glass material properly at a lower temperature (please mention the temperature.

2.5 Preparation of Dye

The dye is prepared from the peel of sesalpina sappan fruit[21]. The collected peel of the fruit is crushed in the mortar till it reaches an absolute semisolid or jelly format. After removing the impurities, with the help of an ether solvent, the liquid form of dye is extracted through filtering from salt paper. The filtered dye is added to the acetone solution. After getting the pure form of Casesalpina sappan dye, the prepared cathode is fully dipped into the dye solution for about 30 minutes.

2.6 Preparation of the redox electrolyte

The solar cell needs free electron flow between the anode and the cathode. The development of free electrons requires a redox couple in the dye-sensitized solar cell. Due to the oxidization and charge pole recombination nature of recombination, free electrons can be generated. This redox couple can be developed from iodide or triodide. The preparation of iodide is explained as follows: The materials needed to establish the iodide are potassium iodide and polyethylene glycol. These two materials are mixed in appropriate amounts. To prepare the 10 mL of the redox couple, the required amounts of potassium iodide, and polyethylene glycol are 0.34 g and 2.965 g, respectively. After mixing these compounds, the mixture is crushed in mortar to reduce the particles' size and make the perfect colloidal mixture. This mixture is taken to 2000 °C for some time to give a redox electrolyte couple[22]

2.7 Preparation of solar cells

In the preparation of a sensitized solar cell, the anode, cathode, and electrolyte are the fundamental components. The preparation of the three components is well described above. The resistance optimized anode is clipped to the electrolyte dipped cathode. This setup is kept at room temperature for one day to get a stable solar cell. During this time, the electrolyte is evenly distributed over the entire inner surface area of the solar cell. To tap the electrical energy, external wires are connected between the anode and cathode. The generation of electromotive force is tested with the multimeter in sunlight. To measure the performance parameters accurately, the developed solar cell was tested on CHI660C electrochemical workstation.

3 Results and Discussion

3.1 Graphene oxide

3.1.1 UV-visible spectra

The UV-visible spectra of the aqueous solution of synthesized graphene oxide are represented in Fig. 1.

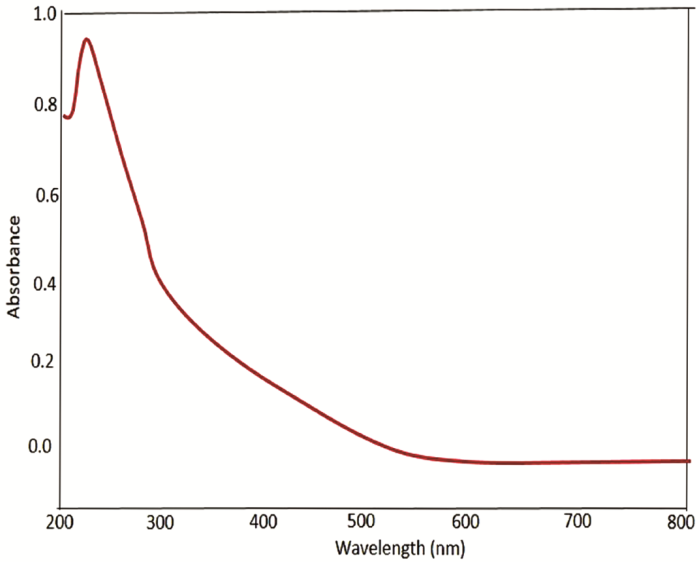

Fig. 1 — UV visible spectra of GO.

It shows the peak that appeared at 232 nm is attributed to π-π* transition of C=C bonds, and the small peak observed at 300 nm is due to the n-π* transition of C=O bonds. These two peaks are in good agreement with those of the graphene oxide sample reported in the literature[19]. From these results, it can be concluded that the overall features of GO samples are identical in nature[23].

3.1.2 X-Ray Diffraction (XRD)

X-ray diffraction (XRD) study of graphene oxide is shown in Fig. 2. It gives detailed information on the degree of oxidation and the layer distances of the starting material and our final product. The typical diffraction peak of our starting graphite was observed at $2\theta = 26.5^{o}$ with a distance layer of 0.34 nm, and the diffraction peak of the final product, graphene oxide, was observed at $2\theta = 11.21^{o}$ with a distance layer of 0.78 nm without reflection at 26.3^{o} from the graphite lattice. From the above results, it is observed that the exfoliation process increased the graphite interlayer spacing by oxidation from 0.34 nm to 0.78 nm[24-25].

3.1.3 Raman Spectra

The Raman spectra of GO are represented in Fig. 3. It shows two bands: one of these G bands at 1589 cm^{-1} is associated with graphitic carbons, and the other strong D-band at 1353 cm^{-1} is related to structural defects or partially disordered graphitic domains, also confirming lattice distortion of graphene basal planes[26].

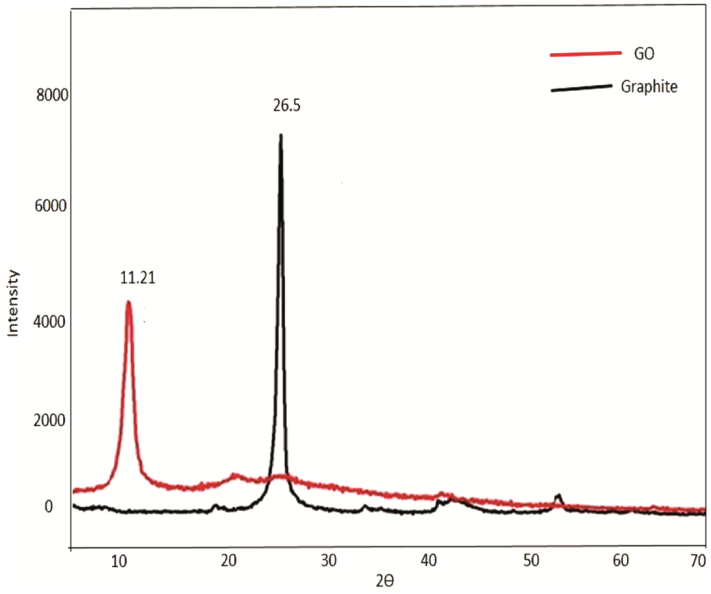

Fig. 2 — XRD of Graphene oxide.

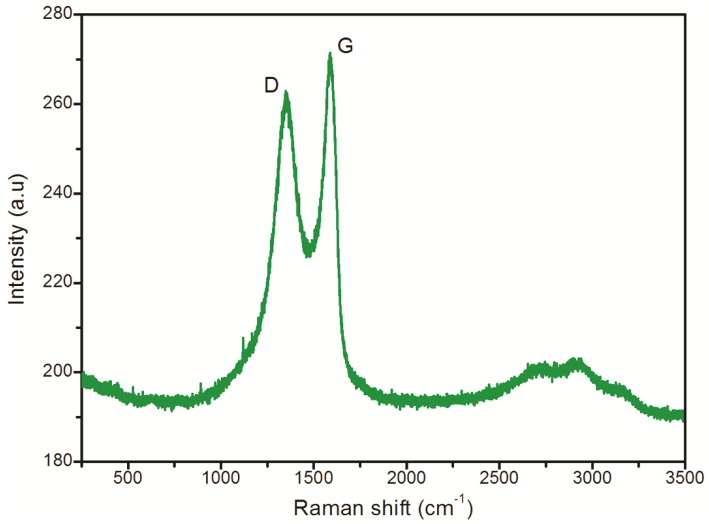

Fig. 3 — Raman spectrum of GO.

3.1.4 FT-IR Spectra

The FT-IR spectra of the synthesized GO are shown in Fig. 4, and it show different characteristic functional groups. The peak observed at 1028 cm^{-1} was due to C-O-C linkages, and the peak that appeared at 1625 cm^{-1} was due to C=C in GO. The broad and strong peak observed at 1755 cm^{-1} is due to the C=O group. The broadband that appeared at 3425 cm^{-1} was observed due to the hydroxyl and carboxyl groups of GO and the water of crystallization associated with GO sheets. The presence of hydrophilic oxygen-containing functional groups gives GO sheets good dispensability in water[27-28].

3.1.5 TGA

To know the thermal stability and functional group information on synthesized graphene oxide, TGA was performed under a nitrogen atmosphere in the range of 49 to 900 °C with a heating rate of 15 °C per minute. The graph is represented in Fig. 5, and it

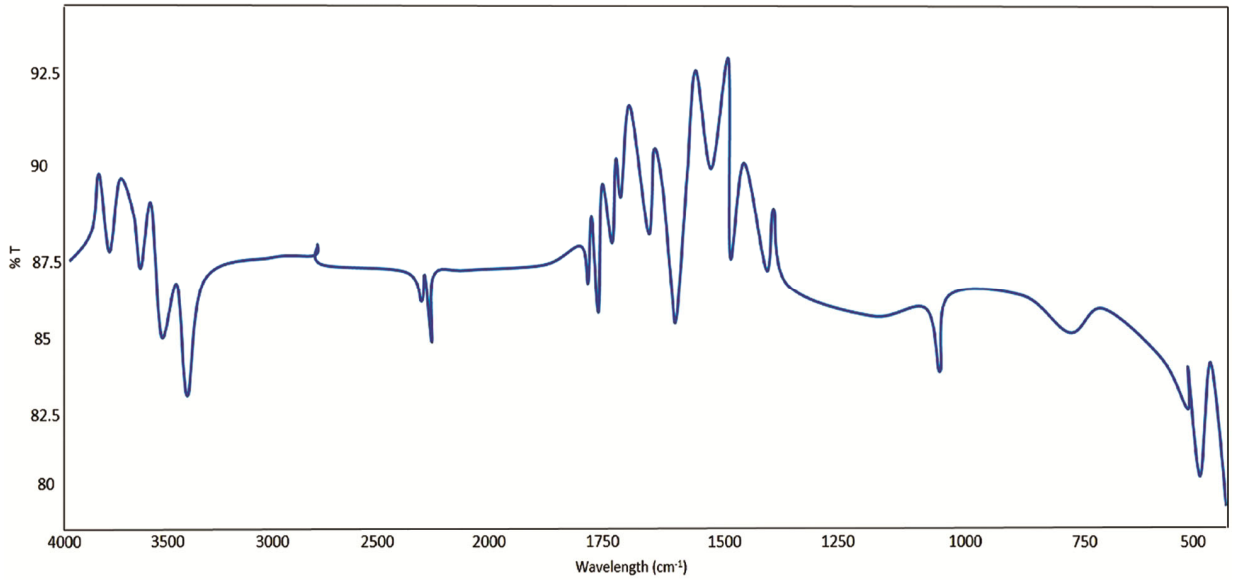

Fig. 4 — FT-IR spectra of GO.

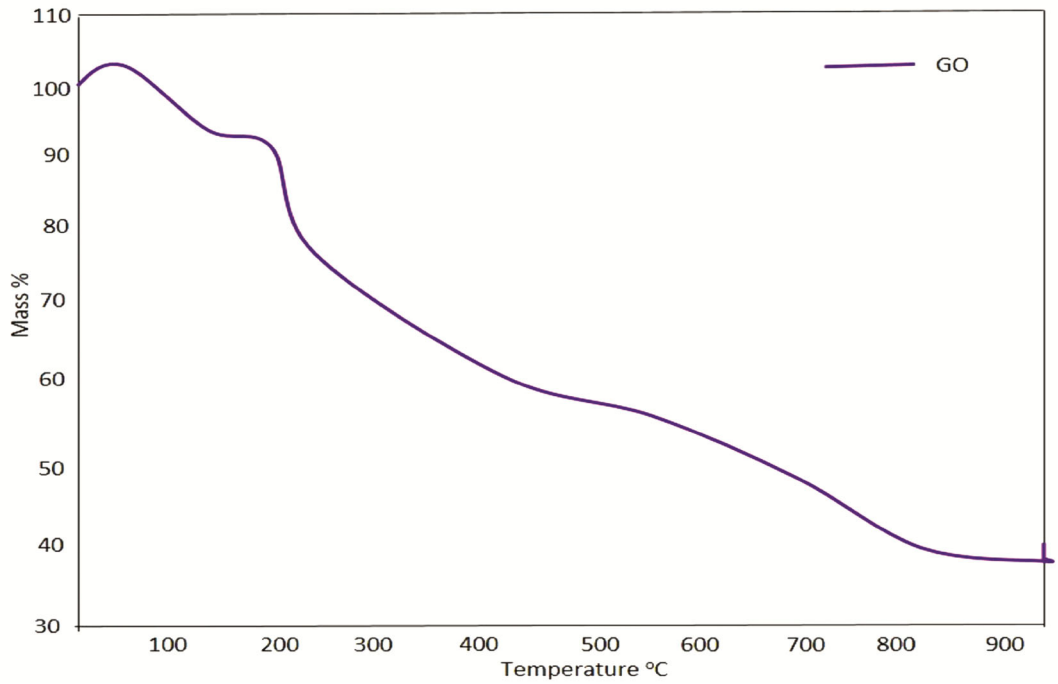

Fig. 5 — TGA curve of GO.

shows that there are three stages of weight loss. The first stage of mass loss includes the removal of the water molecule and epoxy oxygen functional groups before 100 °C, which is called the water of crystallization associated with GO. The second stage of degradation that occurs at 215 °C can be attributed to the removal of phenolic groups, epoxy oxygen, and the decomposition of sp^3 hybridized carbon atoms located at the defective place of GO. The third stage of degradation in the range of 640–900 °C includes very few mass losses of more stable functional groups. [29-31]

3.1.6 SEM

SEM Image of synthesized graphene oxide shown in Fig. 6 From the image, it is seen that the different layers of graphene oxide, show the disassembly of graphite stacks into multiple nanosheets with the appearance of wrinkled paper. These observations can be accounted for by the sp^3 carbons and the formation of oxygen-containing functional groups in the basal planes. The GO has a two-dimensional, sheet-like structure. Figure 6 clearly shows that the synthesized GO has multiple lamellar layers of structures, and it is possible to distinguish the edges of individual sheets from the SEM images. The films are stacked one above another with wrinkled sheeting areas[26,32-33,39].

3.1.7 HR-TEM analysis

To understand and analyse the grain size and surface morphology of the synthesized graphene oxide, HR-TEM analysis is becoming essential. The TEM images shown in Fig. 7 clearly illustrate the crystalline nature of GO sheets. Also, the TEM images exhibit smooth flatness and wideness in the centre of the GO sheets, which are homogeneous. The edges are quite folded and rolled. The lattice fringes are visible on the edges

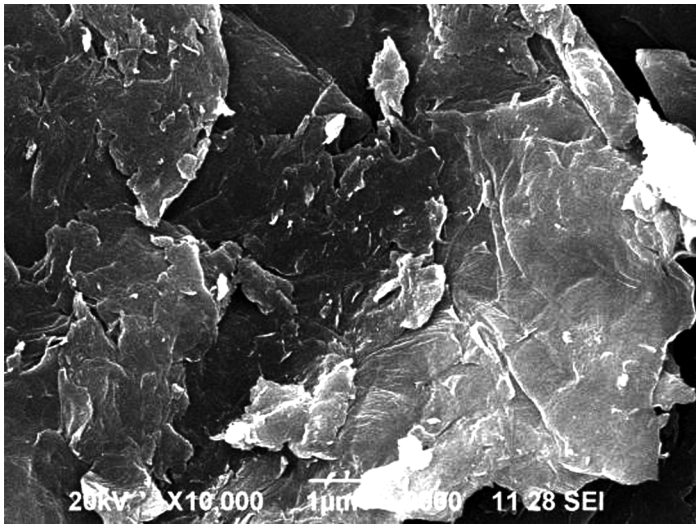

Fig. 6 — SEM Image of GO.

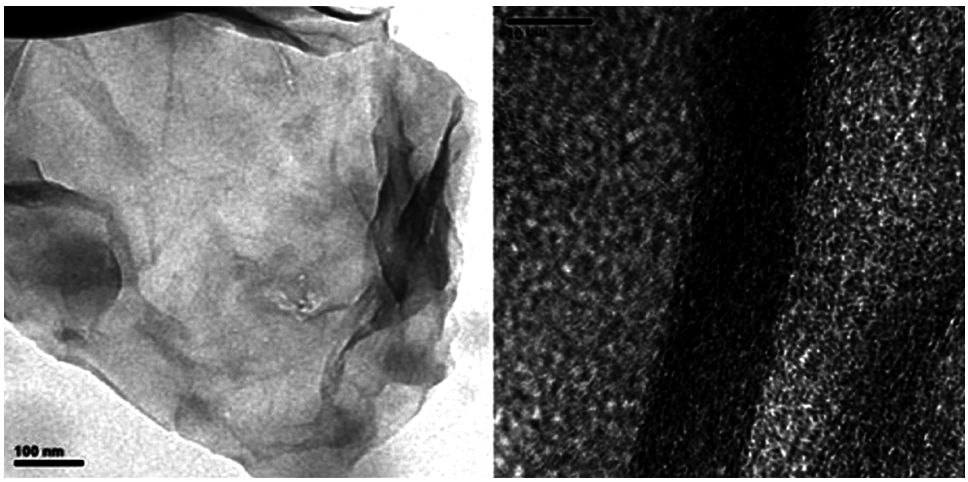

Fig. 7— HR-TEM images of GO.

of GO sheets in the HR-TEM image. The appearance of well-defined diffraction spots is an indication of intercalation on the surface of GO and its crystalline structure.[33-34]

3.2 Optimization of the anode electrode

The synthesized graphene oxide is mixed with water and continuously stirred with a stirrer for up to twenty minutes, and the graphene oxide is fully allowed to disperse. The dispersed solution is taken in a pipet, and it is coated in glass material through the spin coating and sintering further with annealing. The coating process is done at different temperatures, between 100-400 °C. For each coating, the resistance is measured with different coatings and different temperatures. Between 100 °C. and 300 °C. The resistance of the anode is decreasing and increasing exactly as it follows a V-shaped curve. The coating is done up to five times, and the optimum resistance is found at the fourth coating at 240 °C at 143Ω. As we know well, for the preparation of DSSC, the least resistance is required. The measured resistance in every instance is shown in graphical format, as shown in Fig. 8.

3.3 Photovoltaic performances of DSSC

The recombination of charges is happening between the conduction band of the redox couple in the electrolyte and the TiO_2 semiconductor. The electron is excited by the visible region of photon energy.

$2E^-_{cb}+I_3^- \; 3I^-$

Thus, the developed electron from the recombination process can flow through the external electric circuit and be converted into useful heat, electrostatic energy, or electromagnetic energy. At room temperature, the V-I characteristics of the two developed DSSC were measured with the help of a CHI 660C electrochemical workstation [35-36]. The DSSC photovoltaic parameters of current density and open-circuit voltage are derived from V-I characteristics, as shown in Fig. 9. The fill factor and efficiency are calculated as per equations (I) and (II). When we analyse the DSSC, which has lower resistance and higher conductivity, It shows the reduced current density. But the conversion of energy has increased. So that efficiency also increased, followed by a higher fill factor. Table 1 shows the solar cell parameters of efficiency (η), fill factor (FF), open circuit voltage (V_{oc}) and short circuit current density (J_{sc}) with the P_{in} of 82.9 mW/cm^2.[37]

Fill Factor (FF) = ... (I)[38]

Efficiency (η) = ... (II)

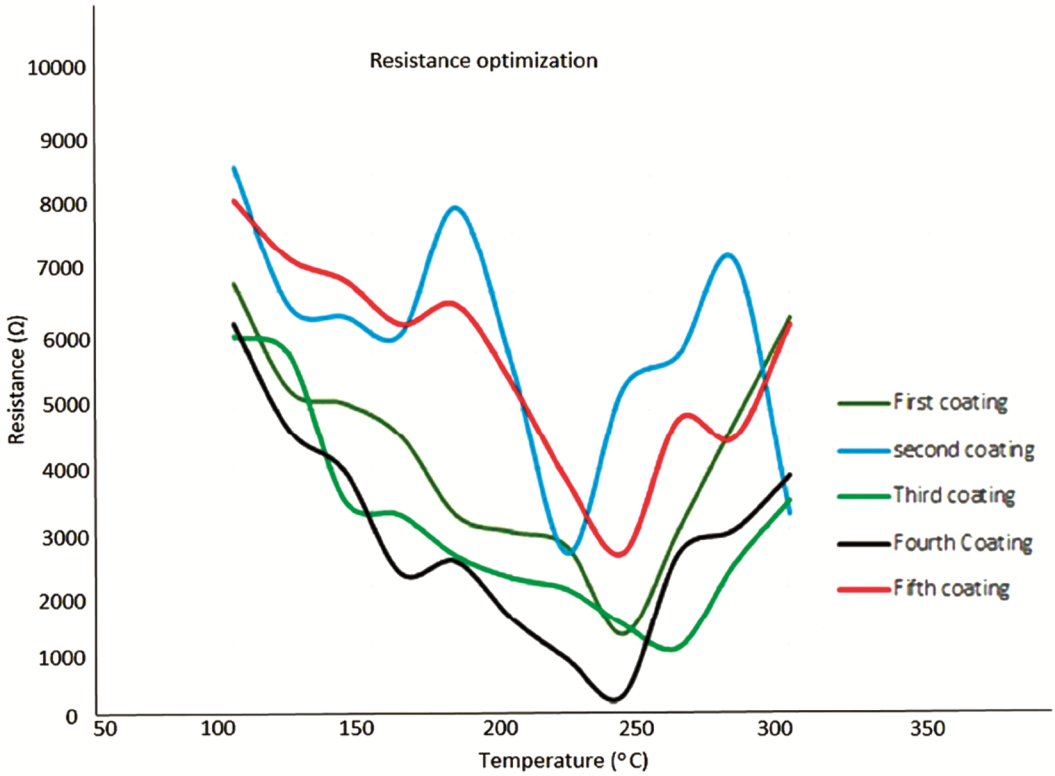

Fig. 8 — Anode resistance optimization.

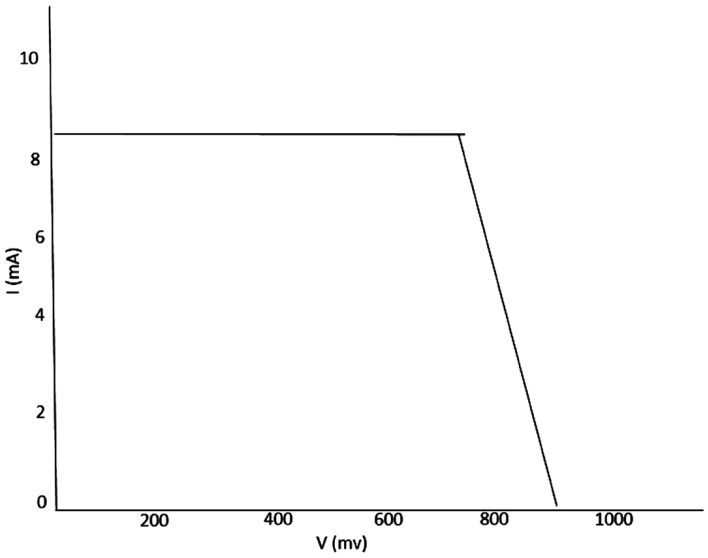

Fig. 9 — V-I Characteristics of optimized anode DSSC.

Table 1 — Efficiency and Fill Factor Calculation

DSSC	Resistance (Ω)	J_{SC} (mA/cm^2)	V_{OC}(mV)	Efficiency (%)	Fill Factor
Anode1	761Ω	9.12	717	5.16	0.64
Anode 2	143Ω	8.72	751	5.61	0.72

The calculated value with the optimized resistance of 143 Ω anode and the other unoptimized anode resistance of 761 Ω is used for developing DSSC as an anode, and the fill factor and efficiency are calculated as follows: The pin is the input of the solar cell, taken from the intensity of the light.

4 Conclusion

The chemical process of the Hummers method produces the oxide ceramic of GO. And it has been confirmed by various characterization techniques. Since the DSSC is exposed to sunlight, thermal stability is essential in the synthesized material. So the thermal stability of the synthesized GO is checked by TGA. From TEM and SEM analysis, multi-layered, thinly stacked flakes' structure and particle size are determined and studied. After the conformation, the synthesized GO is coated in the glass anode of DSSC and it is converted into RGO by direct heating and sintering. The resistance of the anode is optimized with increasing temperature and the number of coatings. With the optimized anode, DSSC is successfully prepared with an efficiency of 5.61%.

References

1 Georgakilas V, *Chem Rev*, 112 (11) (2012) 6156.
2 Montes Navajas P, Asenjo N G, Santamaría R R, A Corma, and García H, *Langmuir*, 2944 (2013) 13443.
3 Son S Y, *ACS Appl Mater Interfaces*, 11 (2019) 13616.
4 Wang S, Ang P K, Wang Z, Tang A L L, Thong J T L, and Loh K P, *Nano Lett*, 10 (2010) 92.
5 Shen C, Barrios E, and Zhai L, *ACS Omega*, 3 (2018) 4006.
6 Memarian F, Fereidoon A, and Ganji M D, *Superlattices Microstruct*, 2015.
7 Slyusarev Y K, Braga A V, and Slyusarev I Y, *Met Sci Heat Treat*, 59 (2017) 334.
8 Amalraj S and Michael P A, *Results Phys*, 15 (2019) 102797.
9 Fredderics A, *Int J Power Electron Drive Syst*, 4 (2014) 538.
10 Li Y, Cai W, and Wang C, *Energy Procedia*, 105 (2017) 3440.
11 Meng L, You J, and Yang Y, *Nat Commun*, 9 (2018) 1.
12 Sharma K, Sharma V, and Sharma S S, *Nanoscale Res Lett*, 13 (2018).
13 Karthick S N, Hemalatha K V, Balasingam S K, Manik Clinton F, Akshaya S, and Kim H J, *Interfacial Eng Funct Mater Dye Sol Cells,* (2019) 1.
14 Wu J, *Chem Soc Rev*, 46 (2017) 5975.
15 Kim J K, *Small*, 13(42) (2017) 1.
16 Prakash S K, Singh H, Panjiar H, Manhas S, and Daniel B S S, *Adv Mater Res*, 585 (2012) 255.
17 Marcano D C, *ACS Nano*, 4 (2010) 4806
18 Hummers W S and Offeman R E, *J Am Chem Soc*, 80(6) (1958) 1339.
19 Ramesh P, Amalraj S, Arunachalam P, Gopiraman M, Al-Mayouf A M, and Vasanthkumar S, *Synth Met*, 272 (2020) 116656.
20 Pugalenthi R, *Chem Sci Eng Res*, 1 (2019) 8.
21 Selvarajan S, Jerry J, Dakshinamurthy A, Ramasubbu A, and Mosae Selvakumar P, *Adv Mater Res*, 1086 (2015) 68.
22 Devadiga D, *J Solid State Electrochem*, 25 (4) (2021) 1461.
23 Vacchi I A, Ménard-Moyon C, and Bianco A, *Phys Sci Rev*, 2 (2017) 1.

24 Radey H H, Al-Sawaad H Z, and Khalaf M N, *Graphene*, 07 (2018) 17.
25 Manza H T, Dhore M S and Amalraj S, *ECS Transaction,* 107 (1) (2021) 16531.
26 Oh W C and Zhang F J, *Asian J Chem*, 23 (2011) 875.
27 Dhore M S, Butoliya S S, and Zade A B, *ISRN Polym Sci*, (2014) 1
28 Yan J, Zhang Y Kim P, and Pinczuk A, *Phys Rev Lett*, 98(16) (2007) 1.
29 Dhore M S, Butoliya S S, and Zade A B, *J Indian Chem Soc*, 92(1) (2015)147.
30 Activity I A, T k G, Harish G, Chamundeeswari D, and Reddy C U, *Sci York,*1 (782) 782.
31 Belsare P U, Zade A B, and Dhore M S, *Res J Pharm Biol Chem Sci*, 6(2) (2015) 1284.
32 Jin Z, Yao J, Kittrell C, and Tour J M, *ACS Nano,* 5(5) (2011) 4112.
33 Szabó T, *Chem Mater,*18(11) 2740 (2006).
34 T soufis T, Tuci G, Caporali S, Gournis D, and Giambastiani G, *Carbon N Y*, 59 (2013).
35 Xuhui S, Xinglan C, Wanquan T, Dong W, and Kefei L, *AIP Adv*, 4(3) (2014)
36 Pan M, Huang N, Zhao X, Fu J, and Zhong X, *J Nanomater,* (2013.
37 Takagi K, Magaino S, Saito H, Aoki T, and Aoki D, *J Photochem Photobiol C Photochem Rev*, 14(1) (2013) 1.
38 Erten-Ela S, *Int J Photoenergy*, (2014).
39 Nagababu P & Maskare D & Kularkar A & Aquatar Md & Rayalu S & Krupadam R *Environmental Nanotechnology, Monitoring, and Management,* 16 (2021) 100545.